The Effects of Tilt on Interferometric Rotation Sensors

by N. D. Pham, H. Igel, J. Wassermann, A. Cochard, and U. Schreiber

Abstract Ring-laser rotation sensors are contaminated by rotations around horizontal axes (also called tilts) through the vector product between the local normal direction and the vector of the rotation rate composed of Earth's rotation and local ground rotations. In this study, we investigate theoretically this cross-axis sensitivity and estimate the effects based on magnitude–amplitude relations to be expected for observations of local earthquakes and teleseismic events. We investigate tilt-ring-laser coupling for rotational motions in the *P* coda of several past earthquakes using tilt motions derived from observed translations. The results show that compared to the corresponding vertical rotation rate tilt-ring-laser coupling is negligible for observations of teleseismic events and for the applicable range of the local magnitude scale.

Introduction

With ring-laser technology seismologists can now observe rotational ground motions for a wide magnitude and distance range (Pancha *et al.*, 2000; Igel *et al.*, 2005; Schreiber *et al.*, 2005, 2006; Igel *et al.*, 2007). Amplitudes of ring-laser rotational signals are used to estimate phase velocities (Igel *et al.*, 2007) or constrain subsurface properties (Fichtner and Igel, 2008; Pham *et al.*, 2009). Moreover, amplitude and waveform modeling of rotational motions requires quantitative understanding of all factors contributing to the signals. Therefore, each effect that contributes to ring-laser measurements has to be considered carefully.

Although ring-laser rotation sensors are built to be insensitive to translations, their records are contaminated by horizontal components of rotations or coseismic tilts (McLeod *et al.*, 1998; Schreiber *et al.*, 2005, 2006, 2009). Tilt-ring-laser coupling, therefore, may potentially contribute to ring-laser measurements. However, this effect has so far not been looked at in a quantitative way or in connection with observed rotations. In addition, previous rough estimates of tilt-ring-laser coupling were erroneously based on tiltmeter measurements that are primarily sensitive to horizontal acceleration in the frequency band considered.

The main goal of this study is to investigate quantitatively the effects of coseismic tilts on ring-laser measurements. While the problem in itself deserves attention, the main motivation for the present study comes from observation of rotational motions in the *P* coda (Igel *et al.*, 2007; Pham *et al.*, 2009). In order to understand the origin of these signals all potential contributions need to be quantified. In the present study the focus is on tilt-ring-laser coupling in general with specific applications to local and teleseismic events. The tilt-ring-laser coupling is evaluated based on the comparison with the corresponding vertical rotation rate. Thus, the so-called significant (or negligible) tilt-ring-laser coupling in this study means the tilt-ring-laser coupling are significant (or negligible) compared to the corresponding vertical rotation rate.

We first investigate theoretically tilt-ring-laser coupling and perform estimates of the effects based on magnitude–amplitude relations to be expected for observations of local earthquakes and teleseismic events. We then apply the theory to the observations in the *P* coda. We estimate tilt-ring-laser coupling in the *P* coda of several observed events based on translation derived tilts (Li *et al.*, 2001). We conclude that the effects can be neglected for observations of teleseismic events and for the applicable range of the local magnitude scale.

Tilt-Ring-Laser Coupling: Theory

Ring-laser sensors allow us to observe rotational ground motions with high accuracy through the Sagnac effect (Schreiber *et al.*, 2005, 2006; Igel *et al.*, 2007):

$$\Delta f = \frac{4A}{\lambda P} \mathbf{n}_R \cdot \dot{\mathbf{\Omega}}, \qquad (1)$$

where A, P, and $\mathbf{n}_R$, respectively, are area, perimeter, and normal unit vector of the ring laser, $\dot{\mathbf{\Omega}}$ is the vector of the imposed rotation rate, λ is the laser wavelength, and Δf is the Sagnac frequency.

Equation (1), called the Sagnac equation, demonstrates that there are three contributions that influence the Sagnac frequency Δf: (1) changes of the scale factor $\frac{4A}{\lambda P}$ under the effects of seismic deformation, temperature variation of the medium, *et cetera*, because the mechanical instrument was extremely rigid and stable, the effects of the scale factor can be avoided (Schreiber *et al.*, 2006); (2) variations in $\dot{\mathbf{\Omega}}$ itself; and (3) changes in the orientation of $\mathbf{n}_R$, when the sensor is tilted by seismic waves and as a result of the inner prod-

uct, it changes the Sagnac frequency (McLeod *et al.*, 1998; Schreiber *et al.*, 2006). This phenomenon called tilt-ring-laser coupling, tilt coupling, or tilt effects will be investigated in the following as it is a potential cause for ring-laser signals in the *P* coda reported by Igel *et al.* (2007) and Pham *et al.* (2009).

To quantify the tilt-ring-laser coupling, we look at equation (1) in detail. As mentioned by McLeod *et al.* (1998), $\dot{\boldsymbol{\Omega}}$ contains both contributions of the Earth's rotation rate and the seismically induced rotation rate. On the surface of the Earth, the seismically induced rotation rate can be expressed by three orthogonal components (vertical, north–south, and east–west). Thus, (1) can be rewritten as

$$\Delta f = \frac{4A}{\lambda P} \mathbf{n}_R (\dot{\Omega}_P \mathbf{n}_P + \dot{\Omega}_Z \mathbf{n}_Z + \dot{\Omega}_N \mathbf{n}_N + \dot{\Omega}_E \mathbf{n}_E). \quad (2)$$

$\dot{\boldsymbol{\Omega}}$ is the rotation rate of the Earth around its rotation axis. $\dot{\Omega}_Z$, $\dot{\Omega}_N$, and $\dot{\Omega}_E$ are seismically-induced rotation rates around vertical, north–south, and east–west axes, respectively.

The unit basis vectors of the rotation axis of the Earth, vertical, north–south, and east–west axes are $\mathbf{n}_P$, $\mathbf{n}_Z$, $\mathbf{n}_N$, and $\mathbf{n}_E$, respectively.

Expanding the inner product in (2) we have

$$\Delta f = \frac{4A}{\lambda P} [\dot{\Omega}_P \alpha_P + \dot{\Omega}_Z \alpha_Z + \dot{\Omega}_N \alpha_N + \dot{\Omega}_E \alpha_E]. \quad (3)$$

Here α_P, α_Z, α_N, and α_E are cosines of the angles between $\mathbf{n}_R$ and $\mathbf{n}_P$, $\mathbf{n}_Z$, $\mathbf{n}_N$, and $\mathbf{n}_E$, respectively, that can be calculated as the functions of the east–west and north–south horizontal components of seismically induced rotations Ω_E, Ω_N (or coseismic tilts), and the latitude of the ring-laser location Λ (see Appendix A1).

Equation (3) contains the cross-axis sensitivity of a ring laser. In case $\Omega_E = 0$ and $\Omega_N = 0$ (there is no tilt), we will have $\alpha_P = \sin(\Lambda)$, $\alpha_Z = 1$, $\alpha_N = \alpha_E = 0$, and equation (3) simplifies to

$$\Delta f = \frac{4A}{\lambda P} [\dot{\Omega}_P \sin(\Lambda) + \dot{\Omega}_Z]. \quad (4)$$

In several past studies (e.g., Igel *et al.*, 2005; Suryanto *et al.*, 2006; Igel *et al.*, 2007) the coseismic tilts, Ω_E and Ω_N, are assumed negligible for teleseismic events; thus, the observed vertical rotation rates were extracted from the Sagnac frequency according to equation (4). In general, as indicated by equation (3), such inferred rotation rate includes the contribution of tilt coupling. Thus, here we call it the contaminated rotation rate $\dot{\Omega}_{Z(\text{cont.})}$ defined as

$$\dot{\Omega}_{Z(\text{cont.})} = \Delta f \frac{\lambda P}{4A} - \dot{\Omega}_P \sin(\Lambda). \quad (5)$$

Combining (5) and (3) leads to

$$\dot{\Omega}_{Z(\text{cont.})} = \dot{\Omega}_P [\alpha_P - \sin(\Lambda)] + \dot{\Omega}_Z \alpha_Z + \dot{\Omega}_N \alpha_N + \dot{\Omega}_E \alpha_E. \quad (6)$$

In our subsequent calculations, we define tilt-ring laser coupling $\dot{\Omega}_{\text{Tilt}}$ as the difference between the contaminated rotation rate $\dot{\Omega}_{Z(\text{cont.})}$ and purely seismically induced rotation rate $\dot{\Omega}_Z$:

$$\dot{\Omega}_{Tilt} = \dot{\Omega}_{Z(cont.)} - \dot{\Omega}_Z,$$
$$\dot{\Omega}_{Tilt} = \dot{\Omega}_P [\alpha_P - \sin(\Lambda)] + \dot{\Omega}_Z (\alpha_Z - 1) + \dot{\Omega}_N \alpha_N + \dot{\Omega}_E \alpha_E. \quad (7)$$

Equation (7) provides us with tilt-ring-laser coupling to be calculated as a function of coseismic tilts and ring-laser location. We note that, to exactly calculate tilt-ring-laser coupling, together with (7) equation (A9a,b,c,d) needs to be applied. With small coseismic tilts, instead of equation (A9), equation (A10a,b,c,d) can be used, and the scale factors in (7) are approximated as follows:

$$[\alpha_P - \sin(\Lambda)] \approx -\Omega_E \cos\left(\Lambda - \frac{\Omega_E}{2}\right), \quad (8a)$$

$$(\alpha_Z - 1) \approx 0, \quad (8b)$$

$$\alpha_N \approx -\Omega_E, \quad (8c)$$

$$\alpha_E \approx -\Omega_N. \quad (8d)$$

In the following we investigate tilt-ring-laser coupling for observations of local earthquakes and teleseismic events in connection with the corresponding vertical rotation rate.

Observations of Local Earthquakes

In this section we investigate the tilt coupling that local earthquakes may induce. We first start with the local magnitude scale

$$M_L = \log(A) - \log(A_O), \quad (9)$$

where A is the maximum trace amplitude (in millimeters) recorded on a standard short-period seismometer (Wood–Anderson instrument) and $\log(A_O)$ is the calibration function and can be calculated as a function of hypocentral distance Δ (in kilometers) for southern California as follows (Hutton and Boore, 1987):

$$-\log(A_O) = 1.110 \log(\Delta/100)$$
$$+ 0.00189(\Delta - 100) + 3.0. \quad (10)$$

With the magnification factor of the Wood–Anderson instrument being 2080 (see Booth, 2007) from equations (9) and (10), we can estimate the maximum displacement A_L (in meters) that an earthquake magnitude M_L may induce is

$$A_L = 10^{(M_L + \log A_O - 3)}/2080. \quad (11)$$

As introduced by Li *et al.* (2001) in a homogeneous half-space, the *y* component of the coseismic tilt induced by plane harmonic *P* and *SV* waves with the propagation direction in the vertical (x, z) plane can be calculated from the corresponding vertical displacement D_Z by

$$-P \text{ wave}: \quad \Omega_y^P = i\omega \frac{\sin \theta_P}{\alpha} D_Z, \quad (12)$$

$$-SV \text{ wave}: \quad \Omega_y^{SV} = i\omega \frac{\sin \theta_{SV}}{\beta} D_Z, \quad (13)$$

where $\omega = 2\pi/T$, T, θ_P, and θ_{SV}, respectively, are frequency, period, and incident angles of *P* and *SV* waves; α and β are *P*- and *S*-wave velocities, and D_Z is the vertical displacement.

In fact, scattered *SV* waves generated by 3D effects may be involved randomly in the *P* coda. Moreover, both *P* and *SV* waves are predominant in a vertical component. Thus, the separation of *P*- and *SV*-wave types is difficult. To simplify calculations, we consider the maximum tilt to be caused by both *P* and *SV* waves. Such maximum tilt can be inferred from equations (12) and (13) by taking sines of the incident angles with maximum value being 1 and wave velocities with minimum value being β:

$$\Omega_{y\text{-max}}^{P_S V} = i \frac{2\pi}{T\beta} D_Z. \quad (14)$$

Equation (14) indicates that at a given period $\Omega_{y\text{-max}}^{P_S V}$ reaches the maximum amplitude when D_Z reaches the maximum displacement:

$$\Omega_{y\text{-max}}^{P_S V} = \frac{2\pi}{T\beta} D_{Z\text{-max}}. \quad (15)$$

Assuming that the maximum displacement extracted from the local magnitude scale is a representative for vertical displacement (e.g., of *SV*) and letting $T = 0.8$ sec (period of the Wood–Anderson instrument) from (11) and (15), we can estimate the maximum tilt (in radian) induced by a local earthquake of magnitude M_L as follows:

$$\Omega_{y\text{-max}}^{M_L} = \frac{\pi}{832\beta} 10^{(M_L + \log A_O - 3)}. \quad (16)$$

Equation (16) provides us with the maximum transverse tilt to be expected in the domain of local magnitude and distance range. Using this equation, maximum coseismic tilts on bedrock site ($\beta = 3200$ m/sec) and on soft sediment site ($\beta = 500$ m/sec) are calculated for the applicable range of local magnitude. The results are presented in Figures 1 and 3 (left-hand axes). We can see that in the applicable range of local magnitudes ($M_L < 7$) and distance (10 km $\leq \Delta \leq$ 600 km) for both types of ground conditions (sediment and bedrock) the maximum tilt motion is about 10^{-3} rad. This implies that the use of approximations (A10a,b,c,d) and

(8) in this section is well accepted and (7) can be rewritten as

$$\dot{\Omega}_{\text{Tilt}} \approx -\Omega_E \dot{\Omega}_P \cos\left(\Lambda - \frac{\Omega_E}{2}\right) - \Omega_E \dot{\Omega}_N - \Omega_N \dot{\Omega}_E. \quad (17)$$

In theory, *P* and *SV* waves coming with a back azimuth ϕ cause no tilt motion for the radial component. Thus, with the maximum transverse tilt provided by (16) we can calculate the corresponding north–south and east–west components of tilts as follows (see Appendix 2):

$$\Omega_N = -\Omega_{y\text{-max}}^{M_L} \sin(\varphi), \quad (18)$$

$$\Omega_E = \Omega_{y\text{-max}}^{M_L} \cos(\varphi). \quad (19)$$

The corresponding components of maximum tilt rates (in rad/sec) can be estimated using the plane wave assumption

$$\dot{\Omega}_N = \frac{2\pi}{T} \Omega_N = -\frac{2\pi}{T} \Omega_{y\text{-max}}^{M_L} \sin(\varphi), \quad (20)$$

$$\dot{\Omega}_E = \frac{2\pi}{T} \Omega_E = \frac{2\pi}{T} \Omega_{y\text{-max}}^{M_L} \cos(\varphi). \quad (21)$$

Combining (16), (17), (18), (19), (20), and (21), we obtain the maximum tilt coupling $\dot{\Omega}_{\text{Tilt}}^{\max}$ (in rad/sec) as a function of local magnitude and distance as follows:

$$\dot{\Omega}_{\text{Tilt}}^{\max} = \dot{\Omega}_P \frac{\pi}{832\beta} 10^{(M_L + \log A_O - 3)}$$
$$+ \frac{\pi^3}{276889.6\beta^2} 10^{2(M_L + \log A_O - 3)}. \quad (22)$$

We note that factors $[-\cos(\Lambda - \frac{\Omega_E}{2})\cos(\varphi)]$ of the first term and $\sin(\varphi)\cos(\varphi) = \frac{\sin(2\varphi)}{2}$ of the second term in the right-hand side of equation (22) were separately replaced by their maximum values being 1 and 0.5, respectively, and $T = 0.8$ sec.

We estimate the maximum value of the corresponding vertical rotation rate to compare with the aforementioned tilt coupling. Assuming that A_L is representative of *SH*-wave amplitudes, the corresponding peak rotation rate (in rad/sec) can be estimated by using the relationship between displacement and rotation rate (see Igel *et al.*, 2007):

$$\dot{\Omega}_Z = 2\frac{\pi^2}{\beta T^2} A_L = \frac{\pi^2}{665.6\beta} 10^{(M_L + \log A_O - 3)}. \quad (23)$$

Equations (22) and (23), respectively, provide us with maximum tilt-ring-laser coupling and vertical rotation rate to be expected in the domain of local magnitude and distance range. We use these equations to investigate the expected values for two cases, bedrock with $\beta = 3200$ m/sec and soft
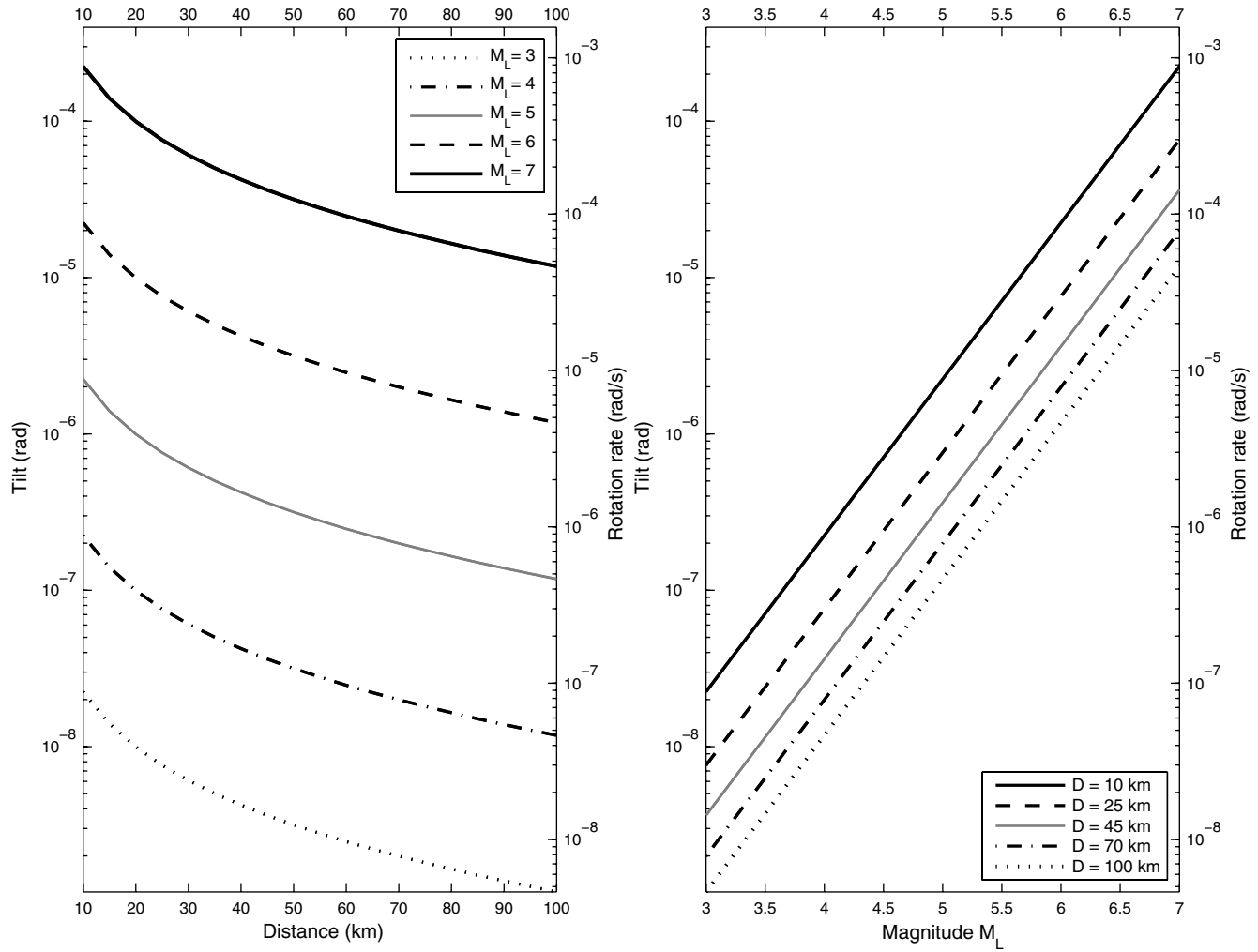
Figure 1. Maximum tilt (left-hand axes) and vertical rotation rate (right-hand axes) are predicted for a dominant period $T = 0.8$ sec on the bedrock ($\beta = 3200$ m/sec) as a function of local magnitude and hypocentral distance.

sediment with $\beta = 500$ m/sec. The results are presented in Figures 1 and 2 (for bed rock) and 3 and 4 (for soft sediment).

The figures show the maximum values to be expected as a function of distance for different magnitudes (left-hand panels) and as a function of magnitude for different distances (right-hand panels). We can see that in the applicable range of local magnitudes ($M_L < 7$) and distance (10 km $\leq \Delta \leq$ 600 km) for both types of ground conditions (sediment and bedrock) at the same distance the increase of one unit of magnitude leads to the enlargement of about one order of amplitude of tilt and rotation rate. The same tendency is shown for tilt-ring-laser coupling at large distances with small magnitude (weak motions). However, at the same distance close to the source with large magnitude (strong motions) the raise of one unit of magnitude results in the increase of about two orders of amplitude of tilt-ring-laser coupling. The maximum tilt-ring-laser coupling predicted for the sediment site is two orders of magnitude bigger than corresponding one on the bedrock. Nevertheless, maximum tilt-ring-laser coupling predicted for both sites (Figs. 2 and 4)

is at least two orders of magnitude smaller than the corresponding maximum rotation rate (right-hand axes of Figs. 1 and 3) and, therefore, can be neglected.

We note that for strong motions at near source, $\dot{\Omega}_Z$, $\dot{\Omega}_N$, and $\dot{\Omega}_E$ may reach amplitudes on the order of 10^{-2} rad/sec (Nigbor, 1994) or greater. This implies that they are much more significant than $\dot{\Omega}_P$ with magnitude on the order of 10^{-5} rad/sec. As a consequence, contribution of the first term in equation (7) can be ignored and the ring-laser location virtually has no effect. In this case, both horizontal components of seismically induced rotations play the same role on affecting ring-laser measurements. At this point it should be noted that ring-laser technology is unlikely to play a major role for near source observations. Nevertheless, other technologies (e.g., fiber-optic approaches) need to be investigated for cross-axis sensitivity in a similar way.

Observations of Teleseismic Events

For teleseismic events $\dot{\Omega}_P$ are much more significant than $\dot{\Omega}_Z$, $\dot{\Omega}_N$, and $\dot{\Omega}_E$ (on the order of 10^{-8} rad/sec for large
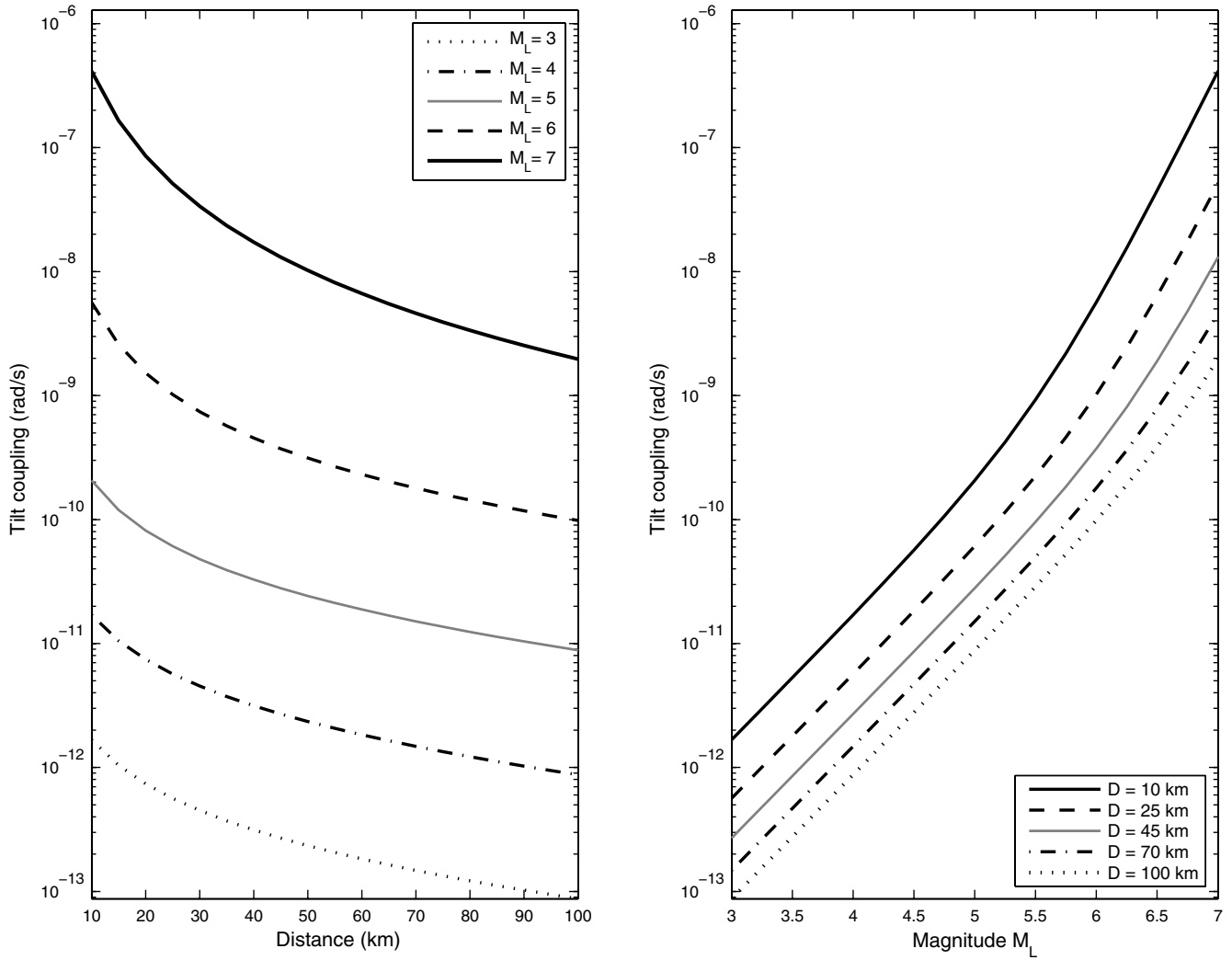
Figure 2. Maximum tilt-ring-laser coupling is predicted for a dominant period $T = 0.8$ sec on the bedrock ($\beta = 3200$ m/sec) as a function of local magnitude and hypocentral distance.

earthquakes, see Igel *et al.*, 2007; Pham *et al.*, 2009). In this case, with scale factors mentioned through equations (8), the significant part of tilt-ring-laser coupling comes from the first term in (7). Thus,

$$\dot{\Omega}_{\text{Tilt}} = -\dot{\Omega}_P \Omega_E \cos\left(\Lambda - \frac{\Omega_E}{2}\right). \qquad (24)$$

Equation (24) implies that for observations of teleseismic events, the tilt coupling depends on the location of the ring laser and Ω_E only. With the same tilt motion, the tilt coupling reaches a maximum when $\Lambda = \Omega_E/2$ (ring laser is almost at the equator) and minimum when $\Lambda = 90$ deg (ring laser at the pole).

We use (24) to investigate the variations of maximum tilt coupling that teleseismic events may induce. We start with the International Association of Seismology and Physics of the Earth's Interior (IASPEI) formula of the surface wave magnitude,

$$M_S = \log(A_S/T) + 1.66 \log D + 3.3, \qquad (25)$$

where A_S is the peak ground amplitude (in micrometers) of the surface (Rayleigh) wave in the vertical component within the period range 18 sec $\leq T \leq 22$ sec, and D is the epicentral distance (in degree) in the range $20° \leq D \leq 160°$.

From (25), Rayleigh waves of an earthquake magnitude M_S are expected to induce a maximum vertical displacement (in meters)

$$A_S = T.10^{(M_S - 1.66 \log D - 9.3)}. \qquad (26)$$

According to Li *et al.* (2002), the coseismic tilt induced by a Rayleigh wave in a homogeneous half-space can be calculated from its vertical displacement D_Z by

$$\Omega_y^R = i\frac{\omega}{V_R}D_Z, \qquad (27)$$

where $\omega = 2\pi/T$ and V_R are frequency and Rayleigh-wave phase velocity, respectively.
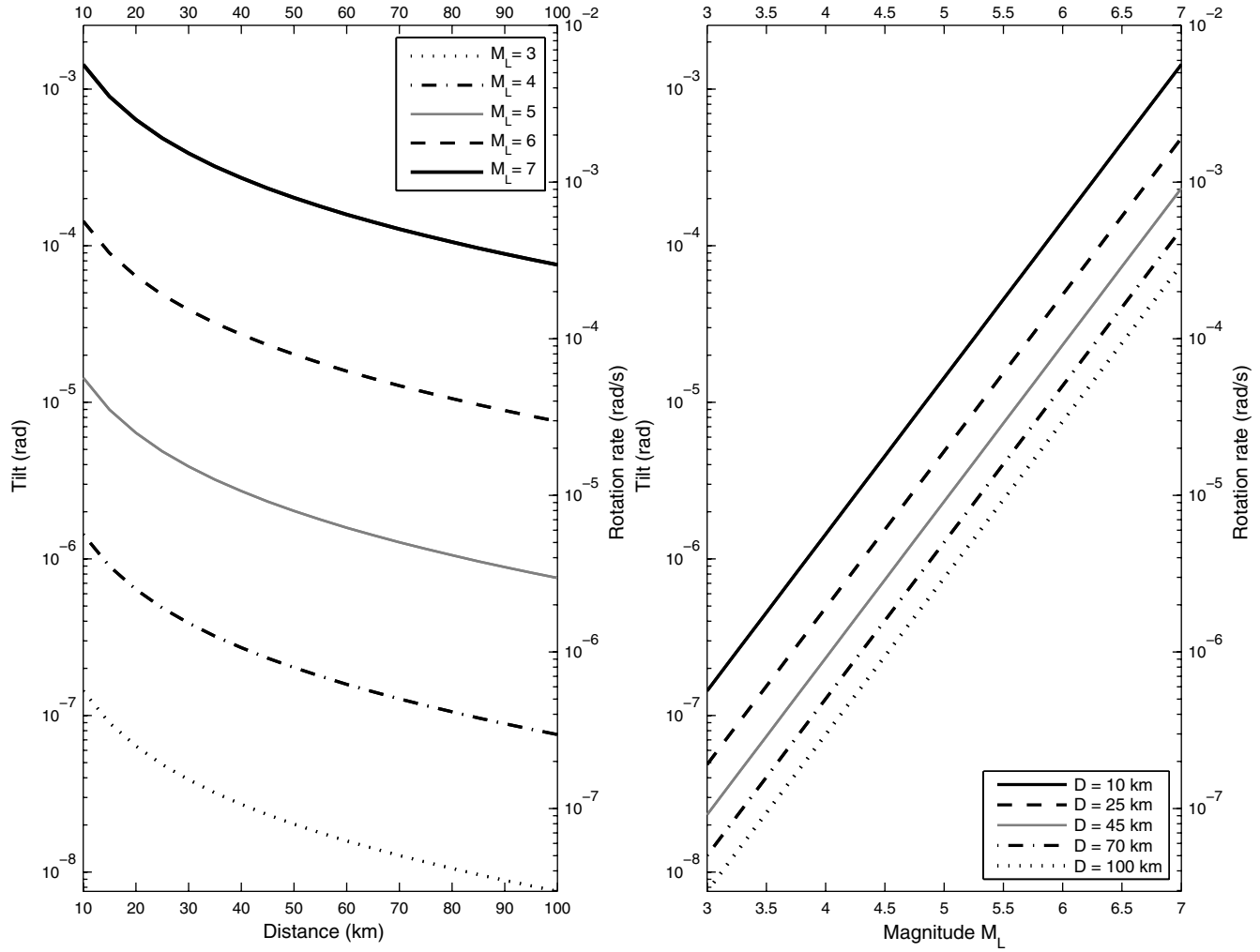
Figure 3. Maximum tilt (left-hand axes) and vertical rotation rate (right-hand axes) are predicted for a dominant period $T = 0.8$ sec on the soft sediment ($\beta = 500$ m/sec) as a function of local magnitude and hypocentral distance.

Equation (27) indicates that with a certain value of the phase velocity at a given period, Ω_y^R reaches the peak value when D_Z reaches a peak displacement A_S,

$$\Omega_y^R\text{-max} = \frac{2\pi}{TV_R} A_S. \tag{28}$$

Combining (26) and (28), the maximum tilt (in radian) induced by an earthquake magnitude M_S, thus, is

$$\Omega_y^R\text{-max} = \frac{2\pi}{V_R} 10^{(M_S - 1.66 \log D - 9.3)}. \tag{29}$$

This Ω_y^R-max will cause maximum tilt-coupling $\dot{\Omega}_\text{Tilt}^R$-max (in rad/sec) if it plays the role of Ω_E in equation (24) and $[-\cos(\Lambda - \frac{\Omega_E}{2})]$ obtains its maximum value being 1,

$$\dot{\Omega}_\text{Tilt}^R\text{-max} = \dot{\Omega}_P \frac{2\pi}{V_R} \cdot 10^{(M_S - 1.66 \log D - 9.3)}. \tag{30}$$

Equations (29) and (30) provide us with the maximum tilt and tilt coupling to be expected in the domain of applicable surface wave magnitude and distance range. Taking $V_R = 3100$ m/sec for a dominant period of $T = 20$ sec, such expected maximum values are calculated and presented in Figure 5. The figure shows the maximum values to be expected as a function of distance for different magnitudes (left-hand panel) and as a function of magnitude for different distances (right-hand panel). The left-hand axes denote the expected tilt in radian and right-hand axes denote the expected tilt coupling in rad/sec. Compared to the corresponding predicted rotation rate shown in Igel *et al.* (2007) the expected tilt coupling is three orders of magnitude smaller and can be ignored.

Tilt-Ring-Laser Coupling: Observations in the *P* Coda

As reported by Igel *et al.* (2007) and Pham *et al.* (2009), there are significant high-frequency motions of vertical component of rotations in the *P* coda of teleseismic signals. This
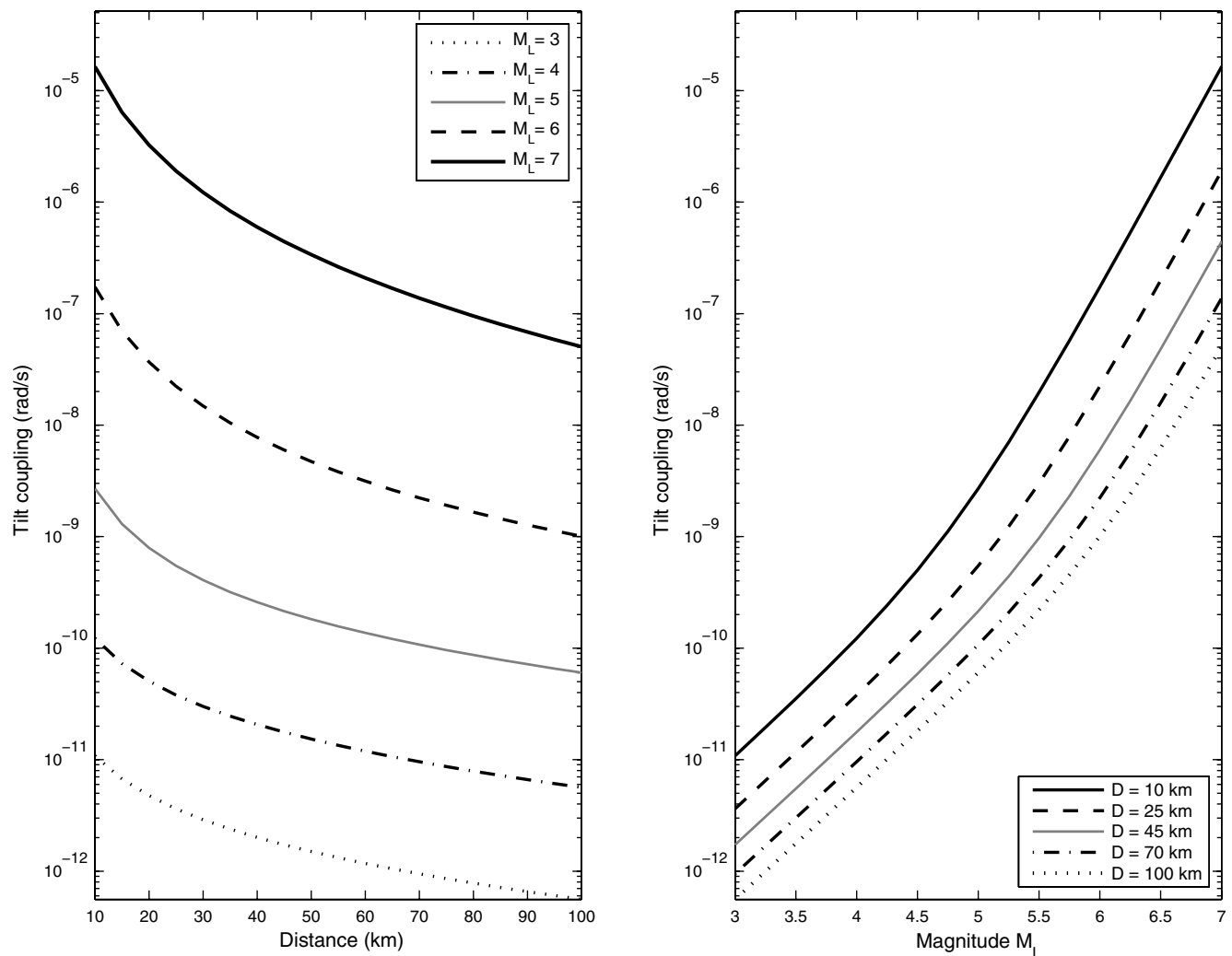
Figure 4. Maximum tilt-ring-laser coupling is predicted for a dominant period $T = 0.8$ sec on the soft sediment ($\beta = 500$ m/sec) as a function of local magnitude and hypocentral distance.

type of signal is either directly visible or can be inferred through the investigation of cross correlation between transverse acceleration and vertical rotation rate. A typical example for this phenomenon is shown in Figure 6 for the 25 September 2003 *M* 8.1 Tokachi-oki event (see Pham *et al.*, 2009, for more details). Theoretically, in spherically symmetric isotropic media, we should not observe a vertical component of rotation before the onset of *SH* waves. One of possible explanations for the observed *P*-coda rotations is tilt-ring-laser coupling. These observations were part of the motivation for the present study aiming at the first quantitative estimates of tilt-ring-laser coupling in connection with teleseismic observations. In this section we focus on investigating the effects of tilt-ring-laser coupling in the observed *P* coda. The aim is to give a quantitative answer to the question of whether tilt-ring-laser coupling contributes to the rotational motions observed in the *P* coda. The magnitude–amplitude relations previously used in the general case do not apply in this case, which is why we estimate the tilt-coupling effects directly from the data.

As shown in the previous section, the calculation of tilt-ring-laser coupling requires knowledge of the horizontal components of seismically induced rotations (or tilts). However, tiltmeters–sensors measuring horizontal components of rotational motions at the Earth's surface are sensitive to translation motions, and therefore, do not provide the correct tilt signals in the required frequency band (Suryanto, 2006). Here we investigate the effects of tilt-ring-laser coupling in the observed *P* coda based on translation derived tilts (see Li *et al.*, 2001).

We apply equation (14) to derive maximum coseismic tilt in the *P* coda from observed translations and use it to quantify the corresponding tilt-ring-laser coupling. It should be noted that Li's equations are developed under the assumption of harmonic plane waves (Li *et al.*, 2001) and a homogeneous half-space. Thus, to derive tilt signal, we first convert the time series of displacements to harmonic discrete frequencies by Fourier transformation. We use equation (14) to define the Fourier spectra of the transverse tilt at discrete frequencies as a function of the Fourier spectra of the displace-
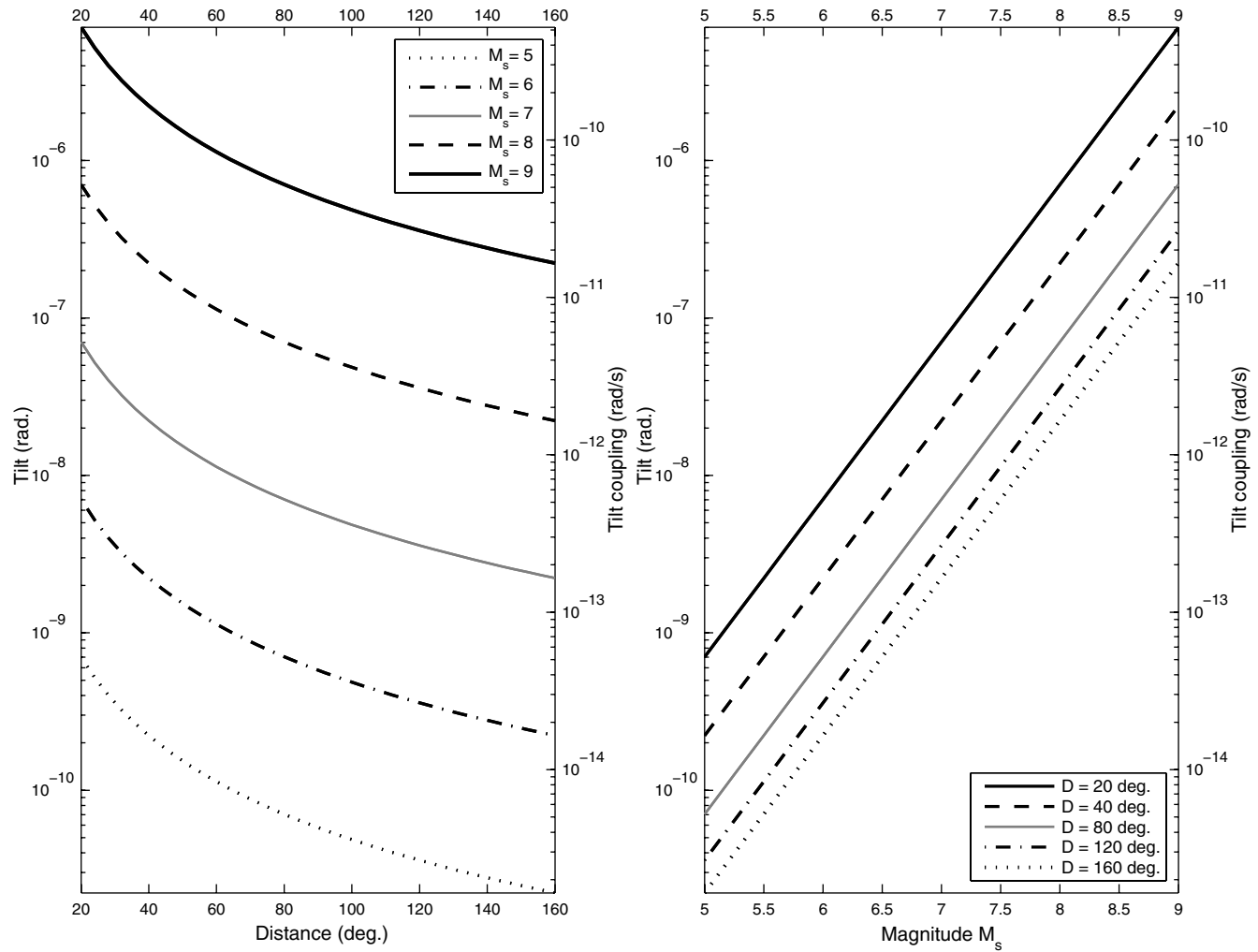
Figure 5. Expected maximum tilt (left-hand axes) and tilt-ring-laser coupling (right-hand axes) induced by teleseismic Rayleigh waves as a function of surface wave magnitude and distance. The phase velocity is assumed to be $V_R = 3100$ m/sec.

ment. The time history of the transverse tilt finally can be obtained by inverse Fourier transformation.

As mentioned by Trifunac *et al.* (2001), Graizer (2005, 2006) and Pillet and Virieux (2007) standard measurements of translations are contaminated by coseismic rotations. Fortunately, this type of contamination is negligible at high frequencies for far field observations. Thus, at high frequencies considered in this study the observed translations are applicable to derive tilt motions.

The observed seismograms of the 25 September 2003 *M* 8.1 Tokachi-oki earthquake are used to investigate tilt-ring-laser coupling in the *P* coda (see the Data and Resources section). The vertical component of the observed velocities of the event is high-pass filtered with a cutoff period of 150 sec, then integrated to obtain displacement. This signal is used to derive the corresponding maximum tilt motion. The translation derived tilt is then applied in the role of the Ω_E in equation (24) to estimate the corresponding tilt-ring-laser coupling. The result is presented in Figure 7 (third trace from top). It is three orders of magnitude smaller than

the corresponding rotation rate measured by the ring-laser sensor; thus, the tilt coupling in the *P* coda of the event is insignificant. In addition, after subtracting this estimated tilt coupling, the *P*-coda rotations are still visible (Fig. 7, fourth trace from top). We calculate zero lag normalized cross-correlation coefficients between the transversal acceleration and the corrected *P*-coda rotations for a 2 sec sliding window after high-pass filtering both signals with a cutoff period of 1 sec. The results show a pronounced increase right after the *P*-wave onset (Fig. 7, bottom trace). All these results indicate that for the observations of the 25 September 2003 *M* 8.1 Tokachi-oki event, the tilt-ring-laser coupling is insignificant and can be ignored.

We finally use the available database of events observed by both the broadband seismometer and the ring-laser sensor at Wettzell station (see the Data and Resources section) to examine systematically maximum tilt-ring-laser coupling in the *P* coda by comparing it with corresponding observed peak rotation rate. Events of 21 May 2003 *M* 6.9 Algeria, 25 September 2003 *M* 8.1 Tokachi-oki, 27 September 2003
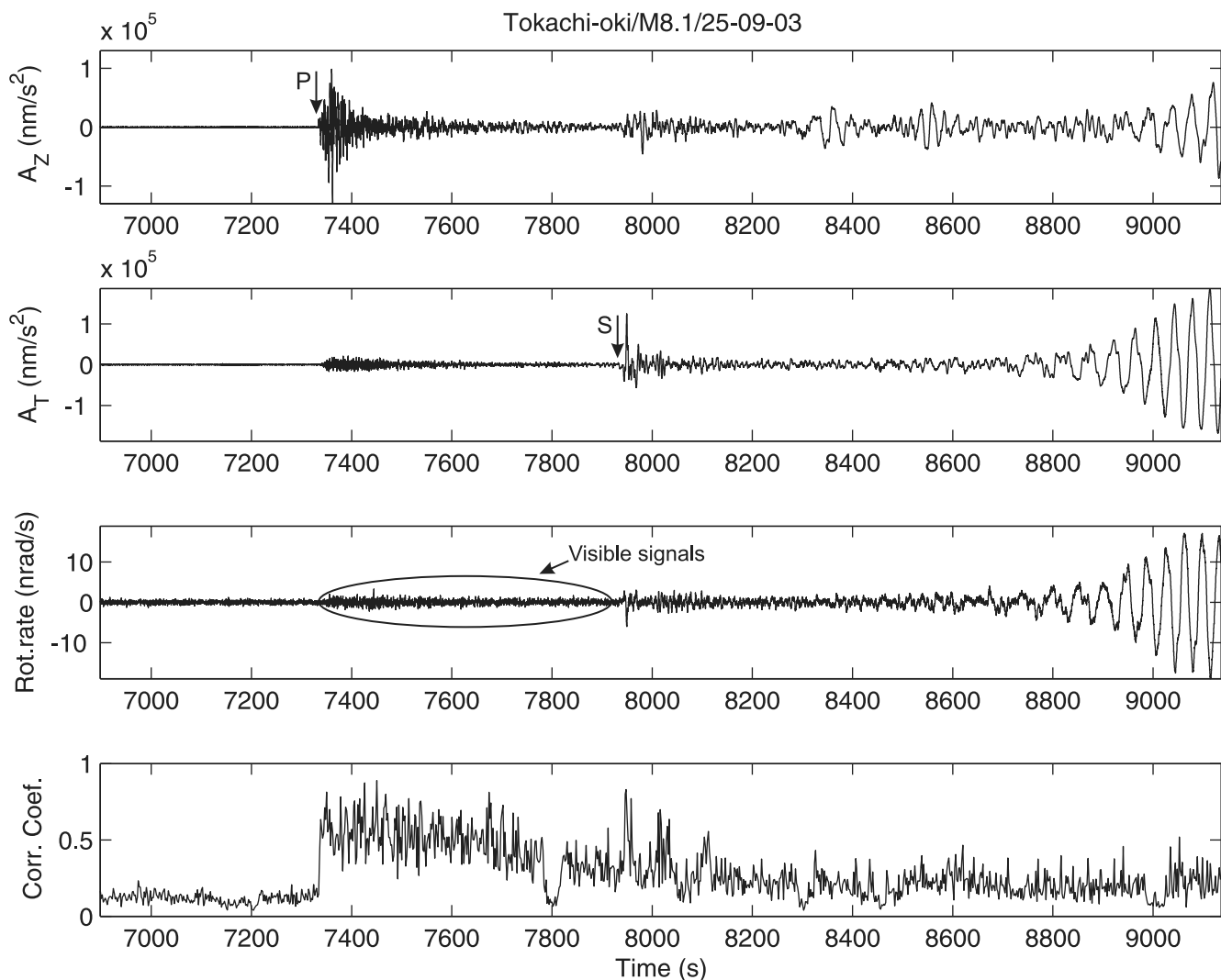
Figure 6. Observations of the 25 September 2003 *M* 8.1 Tokachi-oki event at the Wettzell station. Top three traces: vertical acceleration, transverse acceleration, and rotation rate, respectively. Bottom trace: zero lag normalized cross-correlation coefficients between rotation rate and transverse acceleration after high-pass filtering with cutoff period 1 sec calculated for 2 sec sliding time windows. The figure shows significant rotational motions in the *P* coda.

M 7.5 Russia, and 12 September 2007 *M* 8.4 Sumatra were chosen for this study because they are distributed in different ranges of magnitude, distance, and back azimuth and their *P*-coda rotations are clearly visible (see Pham *et al.*, 2009). Because the observed *P*-coda rotations are predominant around a period of 1 sec (Pham *et al.*, 2009), the vertical displacements and the observed rotation rates of these events are filtered in a narrowband with a central period of 0.5, 1, and 2 sec, and then peak values were extracted. We use equation (15) to calculate maximum coseismic tilt, and then use it as Ω_E in equation (24) to calculate the maximum tilt-ring-laser coupling in the *P* coda. The results are presented in Table 1. We can recognize that for all considered events and periods the predicted tilt-ring-laser coupling is four orders of magnitude smaller than the observed peak rotation rate. We conclude that tilt-ring-laser coupling in the *P* coda is negligible, and the main causes for the observed *P*-coda rotations

thus should come from 3D effects (e.g., *P-SH* scattering as suggested by Pham *et al.*, 2009).

Discussions and Conclusions

Previously, several authors reported about effects of coseismic tilts on ring-laser measurements (e.g., McLeod *et al.*, 1998; Schreiber *et al.* 2005, 2006). However, these studies did not fully quantify the effects and discuss the relevance for broadband ring-laser data processing. The main goal of this study is to fill this gap and investigate quantitatively the effects of coseismic tilts on ring-laser measurements.

In this article, we present equations of cross-axis sensitivity for ring-laser sensors. To calculate tilt-ring-laser coupling requires knowledge of horizontal components of seismically induced rotations (or tilts). Nevertheless, measurements of coseismic tilt using tiltmeters provide incorrect
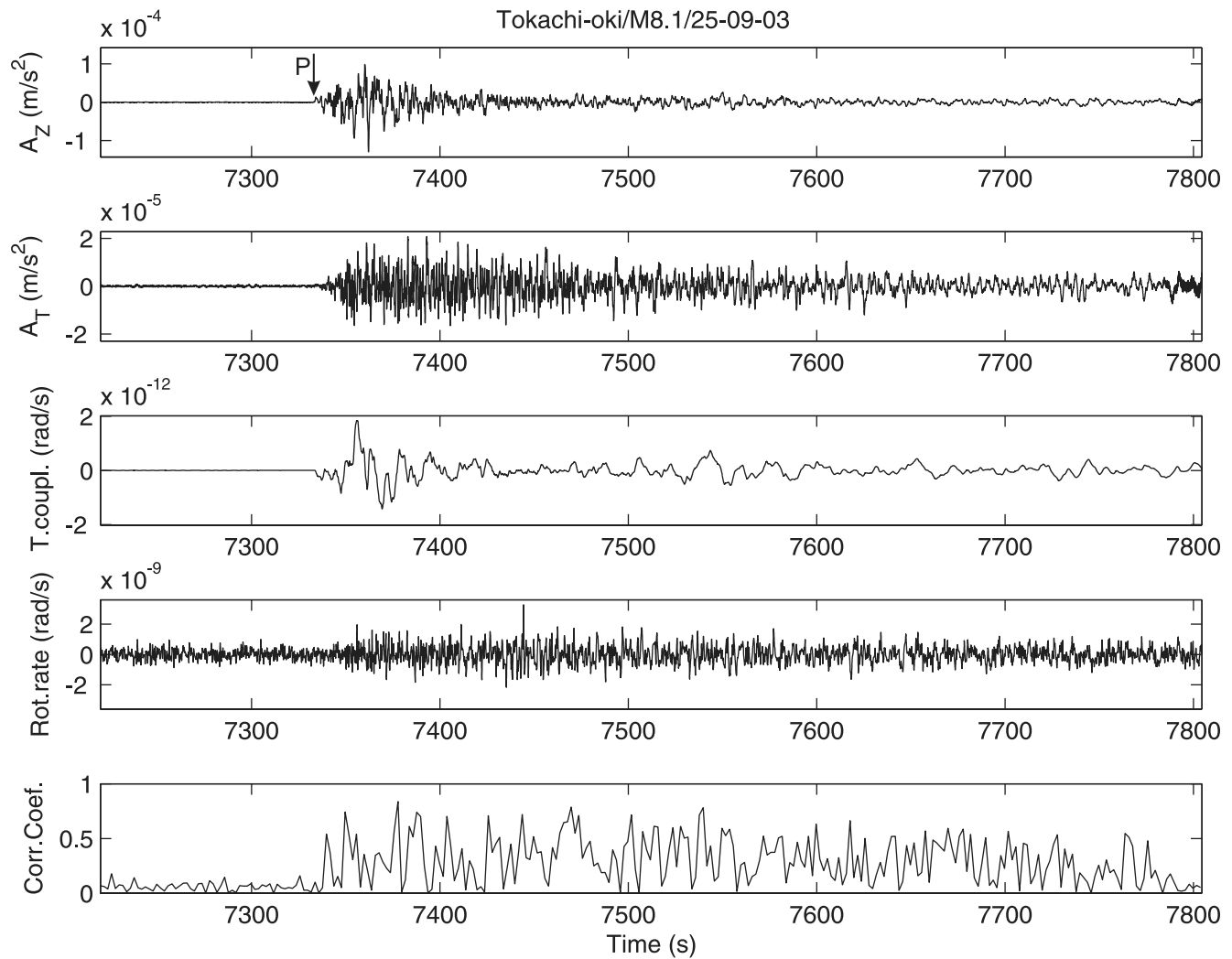
Figure 7. Seismic signals in the *P* coda of the 25 September 2003 *M* 8.1 Tokachi-oki event. Top two traces: vertical (A_Z) and transverse (A_T) components of accelerations; the third trace from the top: the maximum tilt-ring-laser coupling derived from translation; the fourth trace from the top: observed rotation rate after subtracting the maximum tilt-ring-laser coupling; bottom trace: variations of the correlation coefficients between the corrected rotation rate and transverse acceleration.

signals in the frequency band of interest because of the sensitivity of tiltmeters to horizontal accelerations (e.g., Suryanto, 2006). We perform estimates of maximum tilt-ring-laser coupling based on magnitude–amplitude relations to be expected for observations of local earthquakes and teleseismic events. The results show negligible tilt coupling for all the applicable range of the surface wave magnitude and local magnitude scales.

Table 1

Observations and Maximum Tilt and Tilt Coupling at Different Dominant Periods in the *P* Coda of the Typical Events

Event	Observed Peak D_Z (nm)			Observed Peak $\dot{\Omega}_Z$ (nrad/sec)			Maximum Tilt (nrad)			Maximum Tilt Coupling (10^{-5} nrad/sec)		
	0.5 (sec)	1 (sec)	2 (sec)	0.5 (sec)	1 (sec)	2 (sec)	0.5 (sec)	1 (sec)	2 (sec)	0.5 (sec)	1 (sec)	2 (sec)
Algeria 21 May 2003, *M* 6.9	84.40	329.31	631.52	0.14	0.30	0.11	0.31	0.61	0.58	1.50	2.94	2.81
Tokachi-oki 25 September 2003, *M* 8.1	199.52	355.78	1235.37	0.52	0.63	0.44	0.73	0.66	1.14	3.56	3.17	5.51
Russia 27 September 2003, *M* 7.5	73.40	366.53	638.02	0.40	0.46	0.37	0.27	0.68	0.59	1.31	3.27	2.84
Sumatra 12 September 2007, *M* 8.4	75.74	309.34	1353.02	0.07	0.30	0.51	0.28	0.57	1.25	1.35	2.76	6.03

Because ring-laser technology is unlikely to play a major role for near source observations and the appearance of the ring-laser rotational signals in the *P* coda of the teleseismic events (Igel *et al.*, 2007, Pham *et al.*, 2009) needs to be explained, our investigations on data-based tilt-ring-laser coupling focus on the *P*-coda observations. Translation derived tilt (Li *et al.*, 2001) is applied to observed translations to estimate the maximum tilt-ring-laser coupling for *P* coda at high frequencies. The results obtained again show that the tilt-ring-laser coupling can be neglected.

In summary, it can be concluded that tilt-ring-laser coupling is negligible compared to the corresponding vertical rotation rate not only for observations of teleseismic events but also for all the applicable range of the local magnitude scale.

Data and Resources

The observed seismograms of period 2003–2004 used in this study were provided by the Geophysics Section, Ludwig Maximilians University Munich and published by Igel *et al.* (2007). The translational and rotational seismograms of the events that occurred after September 2007 can be obtained from the WebDC Integrated Seismological Data Portal (http://www.webdc.eu/arclink/query?sesskey=0841ed49, last accessed March 2008).

Acknowledgments

References

Booth, D. C. (2007). An improved UK local magnitude scale from analysis of shear and *Lg*-wave amplitudes, *Geophys. J. Int.* **169,** 593–601, doi 10.1111/j.1365-246X.2006.03324.x.

Cochard, A., H. Igel, B. Schuberth, W. Suryanto, A. Velikoseltsev, U. Schreiber, J. Wassermann, F. Scherbaum, and D. Vollmer (2006). Rotational motions in seismology: theory, observations, simulation, in *Earthquake Source Asymmetry, Structural Media and Rotation Effects* R. Teisseyre, M. Takeo, and E. Majewski (Editors), Springer-Verlag, New York, 391–412.

Fichtner, A., and H. Igel (2008). Sensitivity densities for rotational ground motion measurements, *Bulls. Seismol. Soc. Am.* **99,** 1302–1314.

Graizer, V. M. (2005). Effect of tilt on strong motion data processing, *Soil Dyn. Earthq. Eng.* **25,** 197–204.

Graizer, V. M. (2006). Equation of pendulum motion including rotations and its implications to the strong-ground motion, in *Earthquake Source Asymmetry, Structural Media and Rotation Effects*, R. Teisseyre, M. Takeo, and E. Majewski (Editors), Springer-Verlag, New York, 471–491.

Hutton, L. K., and D. M. Boore (1987). The M_L scale in southern California, *Bull. Seismol. Soc. Am.* **77,** 2074–2097.

Igel, H., A. Cochard, J. Wassermann, A. Flaws, U. Schreiber, A. Velikoseltsev, and N. D. Pham (2007). Broadband observations of earthquake induced rotational ground motions, *Geophys. J. Int.* **168,** 182–196, doi 10.1111/j.1365-246X.2006.03146.x.

Igel, H., K. U. Schreiber, A. Flaws, B. Schuberth, A. Velikoseltsev, and A. Cochard (2005). Rotational motions induced by the *M* 8.1 Tokachi-oki earthquake, September 25, 2003, *Geophys. Res. Lett.* **32,** L08309, doi 10.1029/2004GL022336.

Li, H., L. Sun, and S. Wang (2001). Improved approach for obtaining rotational components of seismic motion, *Transactions*, SmiRT **16,** 1–8.

Li, H., L. Sun, and S. Wang (2002). Frequency dispersion characteristics of phase velocities in surface wave for rotational components of seismic motion, *J. Sound Vib.* **258,** no. 5, 815–827.

McLeod, D. P., G. E. Stedman, T. H. Webb, and U. Schreiber (1998). Comparison of standard and ring laser rotational seismograms, *Bull. Seismol. Soc. Am.* **88,** 1495–1503.

Nigbor, R. L. (1994). Six-degree-of-freedom ground-motion measurement, *Bull. Seismol. Soc. Am.* **84,** 1655–1669.

Pancha, A., T. H. Webb, G. E. Stedman, D. P. McLeod, and U. Schreiber (2000). Ring laser detection of rotations from teleseismic waves, *Geophys. Res. Lett.* **27,** 3553–3556.

Pham, N. D., H. Igel, J. Wassermann, M. Käser, J. de la Puente, and U. Schreiber (2009). Observations and modeling of rotational signals in the *P* coda: constraints on crustal scattering, *Bull. Seismol. Soc. Am.* **99,** no. 2B, 1315–1332.

Pillet, R., and J. Virieux (2007). The effects of seismic rotations on inertial sensors, *Geophys. J. Int.* **171,** no. 3, 1314–1323, doi 10.1111/j.1365-246X.2007.03617.x.

Schreiber, K. U., J. N. Hautmann, A. Velikoseltsev, J. Wassermann, H. Igel, J. Otero, F. Vernon, and J.-P. R. Wells (2009). Ring laser measurements of ground rotations for seismology, *Bull. Seismol. Soc. Am.* **99,** no. 2B, 1190–1198.

Schreiber, U., H. Igel, A. Cochard, A. Velikoseltsev, A. Flaws, B. Schuberth, W. Drewitz, and F. Müller (2005). The GEOsensor project: a new observable for seismology, in *Observation of the System Earth from Space*, Springer, New York.

Schreiber, U., G. E. Stedman, H. Igel, and A. Flaws (2006). Ring laser gyroscopes as rotation sensors for seismic wave studies, in *Earthquake Source Asymmetry, Structural Media and Rotation Effects*, R. Teisseyre, M. Takeo, and E. Majewski (Editors), Springer-Verlag, New York.

Suryanto, W. (2006). Rotational motions in seismology, theory and application, *Ph.D. Thesis*, Ludwig-Maximilians University, Munich (http://edoc.ub.uni-muenchen.de/7850/).

Suryanto, W., H. Igel, J. Wassermann, A. Cochard, B. Schuberth, D. Vollmer, F. Scherbaum, U. Schreiber, and A. Velikoseltsev (2006). First comparison of array-derived rotational ground motions with direct ring laser measurements, *Bull. Seismol. Soc. Am.* **96,** 2059–2071.

Trifunac, M. D., and I. M. Todorovska (2001). A note on the usable dynamic range of accelerographs recording translation, *Soil Dyn. Earthq. Eng.* **21,** 4, 275–286.

Appendix A

Variations of the Normal Unit Vector of a Ring Laser

Under the effects of seismic waves, a ring laser may be both tilted and shifted. As a consequence, its normal unit vector $\mathbf{n}_R$ is varied. Here we quantify this variation through cosines of angles between $\mathbf{n}_R$ and the unit basis vectors $\mathbf{n}_P$, $\mathbf{n}_Z$, $\mathbf{n}_N$, and $\mathbf{n}_E$ of the rotation axis of the Earth, vertical, north–south, and east–west axes at the ring-laser location, respectively. To do that we locate all the mentioned vectors in the Cartesian coordinate system $Oxyz$ at the original loca-

tion O of the ring laser in which Ox, Oy, and Oz, respectively, are corresponding with the local east–west, north–south, and vertical axes (Fig. A1).

$\mathbf{n}_Z$, $\mathbf{n}_N$, and $\mathbf{n}_E$ are defined in $Oxyz$ system by

$$\mathbf{n}_{Z(Oxyz)} = \{0, 0, 1\}, \tag{A1}$$

$$\mathbf{n}_{N(Oxyz)} = \{0, 1, 0\}, \tag{A2}$$

$$\mathbf{n}_{E(Oxyz)} = \{1, 0, 0\}. \tag{A3}$$

The unit basis vector $\mathbf{n}_P$ of the rotation axis of the Earth at first is considered in another Cartesian coordinate system $O'X'Y'Z'$ (root point O' and $O'Z'$, respectively, are the core point and the rotation axis of the Earth; see Fig. A1). In this system, $\mathbf{n}_P$ is determined by

$$\mathbf{n}_{P(O'X'Y'Z')} = \{0, 0, 1\}. \tag{A4}$$

On the other hand, let θ and Λ, respectively, denote colatitude and latitude of the original location of the ring laser (Fig. A1); we have

$$\cos(Ox, O'Z') = 0, \tag{A5a}$$

$$\cos(Oy, O'Z') = \cos\left(\frac{\pi}{2} - \theta\right) = \cos(\Lambda), \tag{A5b}$$

$$\cos(Oz, O'Z') = \cos(\theta) = \sin(\Lambda). \tag{A5c}$$

Applying coordinate transformations and using (A4) and (A5), one can infer the $\mathbf{n}_P$ in the $Oxyz$ system

$$\mathbf{n}_{P(Oxyz)} = \{0, \cos(\Lambda), \sin(\Lambda)\}. \tag{A6}$$
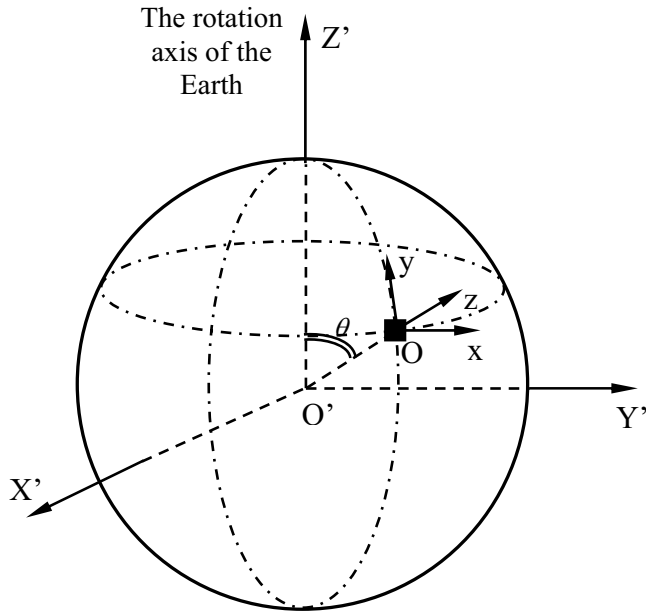

Figure A1. Illustration of ring-laser location on the Earth's surface.

For the normal unit vector $\mathbf{n}_R$ of the ring laser, we locate it from the equation of the ring-laser plane in the $Oxyz$ system, which can be determined through three nonlinear points on the plane (see Appendix C). Assuming that when seismic waves arrive the ring laser is moved to a new certain location $R\{\Delta x, \Delta y, \Delta z\}$ in the $Oxyz$ system (Fig. A2). The seismically induced tilts of the ring-laser sensor about the x and y axes themselves are the horizontal components of rotations Ω_E and Ω_N, respectively (Cochard *et al.*, 2006). Together with R, we choose R_1 in the line of intersection between the ring-laser plane and xOz plane with distance $RR_1 = 1$ and R_2 in the line of intersection between the ring-laser plane and yOz plane with distance $RR_2 = 1$ to determine the equation of the ring-laser plane. The coordinates of R_1 and R_2 in the $Oxyz$ system can be easily determined as $R_1\{\cos(\Omega_N) + \Delta x, \Delta y, \sin(\Omega_N) + \Delta z\}$ and $R_2\{\Delta x, \cos(\Omega_E) + \Delta y, \sin(\Omega_E) + \Delta z\}$ (see Fig. A2). Hence, the equation of the ring-laser plane can be written as follows (Appendix C):

$$\begin{vmatrix} x - \Delta x & y - \Delta y & z - \Delta z \\ \cos(\Omega_N) & 0 & \sin(\Omega_N) \\ 0 & \cos(\Omega_E) & \sin(\Omega_E) \end{vmatrix} = 0$$

or

$$-\cos(\Omega_E)\sin(\Omega_N)x - \sin(\Omega_E)\cos(\Omega_N)y$$
$$+ \cos(\Omega_E)\cos(\Omega_N)z + [\cos(\Omega_E)\sin(\Omega_N)\Delta x$$
$$+ \sin(\Omega_E)\cos(\Omega_N)\Delta y - \cos(\Omega_E)\cos(\Omega_N)\Delta z] = 0. \tag{A7}$$

Equation (A7) implies that changes of location $R\{\Delta x, \Delta y, \Delta z\}$ affect the equation of the ring-laser plane but have no effect on the normal unit vector $\mathbf{n}_R$, which can be inferred as follows (see Appendix C):

$$\mathbf{n}_{R(Oxyz)} = \{n_1, n_2, n_3\}, \tag{A8a}$$

$$n_1 = \frac{-\cos(\Omega_E)\sin(\Omega_N)}{\sqrt{1 - \sin^2(\Omega_E)\sin^2(\Omega_N)}}, \tag{A8b}$$

$$n_2 = \frac{-\sin(\Omega_E)\cos(\Omega_N)}{\sqrt{1 - \sin^2(\Omega_E)\sin^2(\Omega_N)}}, \tag{A8c}$$

$$n_3 = \frac{\cos(\Omega_E)\cos(\Omega_N)}{\sqrt{1 - \sin^2(\Omega_E)\sin^2(\Omega_N)}}. \tag{A8d}$$

Using (A1), (A2), (A3), (A6), and (A8), cosine of angles between normal unit vector $\mathbf{n}_R$ of the ring laser and the unit basis vectors $\mathbf{n}_P$, $\mathbf{n}_Z$, $\mathbf{n}_N$, and $\mathbf{n}_E$ of the rotation axis of the Earth, vertical, north–south, and east–west axes at the ring-laser location, respectively, are calculated by (see Appendix C)
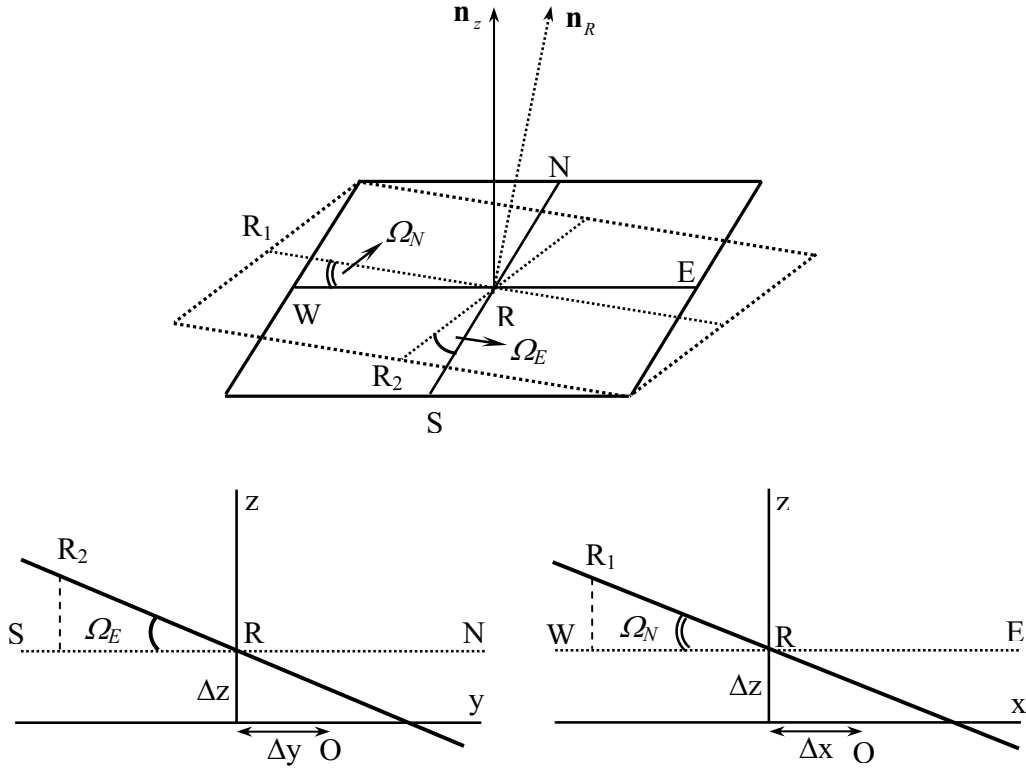
Figure A2. A ring-laser sensor is tilted and shifted by seismic waves. $O\{0, 0, 0\}$ is the original location of the ring-laser. $R\{\Delta x, \Delta y, \Delta z\}$ is the new location of the ring-laser under the effects of a seismic wave. R_1 is chosen in the line of intersection between the ring-laser plane and the xOz plane with distance $RR_1 = 1$. R_2 is chosen in the line of intersection between the ring-laser plane and the yOz plane with distance $RR_2 = 1$.

$$\alpha_P = \frac{\cos(\Omega_N)\sin(\Lambda - \Omega_E)}{\sqrt{1 - \sin^2(\Omega_E)\sin^2(\Omega_N)}}, \qquad \text{(A9a)}$$

$$\alpha_Z = \frac{\cos(\Omega_E)\cos(\Omega_N)}{\sqrt{1 - \sin^2(\Omega_E)\sin^2(\Omega_N)}}, \qquad \text{(A9b)}$$

$$\alpha_N = \frac{-\sin(\Omega_E)\cos(\Omega_N)}{\sqrt{1 - \sin^2(\Omega_E)\sin^2(\Omega_N)}}, \qquad \text{(A9c)}$$

$$\alpha_E = \frac{-\cos(\Omega_E)\sin(\Omega_N)}{\sqrt{1 - \sin^2(\Omega_E)\sin^2(\Omega_N)}}. \qquad \text{(A9d)}$$

In seismology, Ω_E and Ω_N are small. The greatest value of the coseismic tilts that has ever been observed is 4.0×10^{-4} rad (Nigbor, 1994). Thus, we can approximate (A9a, b,c,d) by

$$\alpha_P \approx \sin(\Lambda - \Omega_E), \qquad \text{(A10a)}$$

$$\alpha_Z \approx 1, \qquad \text{(A10b)}$$

$$\alpha_N \approx -\Omega_E, \qquad \text{(A10c)}$$

$$\alpha_E \approx -\Omega_N. \qquad \text{(A10d)}$$

Appendix B

Axis Transformations of Tilts

Assume Cartesian coordinate system NZE is rotated an angle ϕ around Z to another coordinate system, RZT (Fig. B1). To set up the relationship between components of tilt in these coordinate systems, we start with the coordinate relationship between these two systems,

$$\begin{bmatrix} T \\ R \end{bmatrix} = \begin{bmatrix} \cos(\varphi) & -\sin(\varphi) \\ \sin(\varphi) & \cos(\varphi) \end{bmatrix} \begin{bmatrix} E \\ N \end{bmatrix} \qquad \text{(B1)}$$

or

$$T = \cos(\varphi)E - \sin(\varphi)N, \qquad \text{(B2a)}$$

$$R = \sin(\varphi)E + \cos(\varphi)N \qquad \text{(B2b)}$$

or

$$E = \cos(\varphi)T + \sin(\varphi)R, \qquad \text{(B2c)}$$

$$N = -\sin(\varphi)T + \cos(\varphi)R. \qquad \text{(B2d)}$$

Calling U_Z the vertical component of displacement, the components of tilt around N, E, R, and T axes, respectively, are defined by (Cochard *et al.*, 2006)
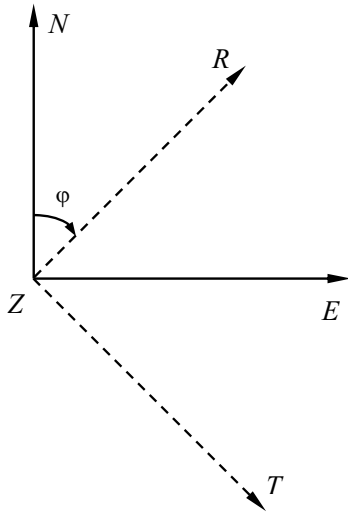
Figure B1. Axis transformations of tilts.

$$\Omega_N = -\frac{\partial U_Z}{\partial E}, \qquad \Omega_E = \frac{\partial U_Z}{\partial N}, \qquad \text{(B3)}$$

$$\Omega_R = -\frac{\partial U_Z}{\partial T}, \qquad \Omega_T = \frac{\partial U_Z}{\partial R}. \qquad \text{(B4)}$$

Now, using the chain rule leads to

$$\Omega_R = -\frac{\partial U_Z}{\partial T} = -\left(\frac{\partial U_Z}{\partial N}\frac{\partial N}{\partial T} + \frac{\partial U_Z}{\partial E}\frac{\partial E}{\partial T}\right), \qquad \text{(B5)}$$

$$\Omega_T = \frac{\partial U_Z}{\partial R} = \left(\frac{\partial U_Z}{\partial N}\frac{\partial N}{\partial R} + \frac{\partial U_Z}{\partial E}\frac{\partial E}{\partial R}\right). \qquad \text{(B6)}$$

From (B2c) and (B2d) we know that

$$\frac{\partial E}{\partial T} = \cos(\varphi), \qquad \frac{\partial E}{\partial R} = \sin(\varphi),$$
$$\frac{\partial N}{\partial T} = -\sin(\varphi), \qquad \frac{\partial N}{\partial R} = \cos(\varphi). \qquad \text{(B7)}$$

Combining (B3), (B5), (B6), and (B7), we have the relationship

$$\Omega_R = \Omega_E \sin(\varphi) - \Omega_N \cos(\varphi), \qquad \text{(B8)}$$

$$\Omega_T = \Omega_E \cos(\varphi) - \Omega_N \sin(\varphi), \qquad \text{(B9)}$$

or

$$\Omega_N = \Omega_R \cos(\varphi) - \Omega_T \sin(\varphi), \qquad \text{(B10)}$$

$$\Omega_E = \Omega_R \sin(\varphi) + \Omega_T \cos(\varphi). \qquad \text{(B11)}$$

Appendix C

Fundamental Formulas

1. The equation of a plane through three given nonlinear points $M_1(x_1, y_1, z_1)$, $M_2(x_2, y_2, z_2)$, $M_3(x_3, y_3, z_3)$ can be determined by

$$\begin{bmatrix} x - x_1 & y - y_1 & z - z_1 \\ x_2 - x_1 & y_2 - y_1 & z_2 - z_1 \\ x_3 - x_1 & y_3 - y_1 & z_3 - z_1 \end{bmatrix} = 0.$$

2. The normal unit vector of a plane $Ax + By + Cz + D = 0$ is expressed by

$$\left\{\frac{A}{\sqrt{A^2 + B^2 + C^2}}, \frac{B}{\sqrt{A^2 + B^2 + C^2}}, \frac{C}{\sqrt{A^2 + B^2 + C^2}}\right\}.$$

3. the cosine of angle between two vectors $\{A_1, B_1, C_1\}$ and $\{A_2, B_2, C_2\}$ can be calculated by

$$\frac{A_1 A_2 + B_1 B_2 + C_1 C_2}{\sqrt{A_1^2 + B_1^2 + C_1^2}\sqrt{A_2^2 + {}_2 B^2 + C_2^2}}.$$

Geophysics Section, Department of Earth and Environmental Sciences
Ludwig Maximilians Universität
Theresienstrasse 41
D-80333 München, Germany
nguyen@geophysik.uni-muenchen.de
heiner.igel@lmu.de
   (N.D.P., H.I.)

Geophysical Observatory
Department of Earth and Environmental Sciences
Ludwig Maximilians Universität
Ludwigshöhe 8, 82256
Fürstenfeldbruck, Germany
joachim.wassermann@geophysik.uni-muenchen.de
   (J.W.)

Ecole et Observatoire des Sciences de la Terre
Institut de Physique du Globe
5 rue Reńe Descartes
F-67084 Strasbourg Cedex
France
Alain.Cochard@eost.u-strasbg.fr
   (A.C.)

Forschungseinrichtung Satellitengeodäsie
Technical University Munich
Fundamentalstation Wettzell
Sackenriederstrasse 25
D-93444 Kötzting, Germany
schreiber@wettzell.ifag.de
   (U.S.)